



9th International Conference on

Fundamental and applied MHD, Thermo acoustic and Space technologies



SEVENTH FRAMEWORK
PROGRAMME

Theme 9: SPACE

Riga – Latvia

June 16-20, 2014



Chairmen A. Alemany France, J. Freibergs, Latvia

Co-chairmen :

J.P. Chopart, France – C. Latge, France – M. Francois, France - E. Gaia, Italy

Secretaries : B. Collovati, France - M. Broka, Latvia

pamir@simap.grenoble-inp.fr



University of Latvia
Institute of Physics



Supporting Organisation

CNRS : Centre National de la Recherche Scientifique
INP : Institut Polytechnique de Grenoble
UJF : Université Joseph Fourier Grenoble
CEA : Commissariat à l'Énergie Atomique
Ministère de l'Enseignement Supérieur et de la Recherche
Ambassade de France à Alger
Ambassade de France à Riga



CONTENTS

VOLUME 2

D. LIQUID METAL TECHNOLOGIES FOR COOLANT APPLICATIONS

D.1. Power generation

D.1.1. - Role of thermoelectromagnetic forces in capillary porous systems proposed for liquid metal cooling of fusion reactor components I. Kaldre, O. Lielausis	1
D.1.2. - Dual-Coolant Lead-Lithium (DCLL) blanket: status and R&D in the area of MHD thermofluids S. Smolentsev, M. Abdou	6
D.1.3. - AMTEC clusters as add-on system for power generation in a concentrated solar power plant A. Onea, N. Diez de los Rios Ramos, J.L. Palacios, W. Hering	11
D.1.4. - Experimental studies of liquid Lithium film flow in magnetic field E. Platacis, A. Sobolev, A. Shishko, F. Muktepavela	16
D.1.5. - LM jet and film flows over solid substrates in strong magnetic fields O. Lielausis, E. Platacis, A. Klukins, J. Peinbergs	20
D.1.6. - Liquid metal in nuclear applications E. Platacis	25

D.2. MHD pumps and flow control

D.2.1. - Ferrous yoke construction influence on permanent magnets pump efficiency I. Buceniaks, K. Kravalis, R. Nikoluskins	29
D.2.2. - A simplified model of centrifugal electromagnetic induction pump with rotating permanent magnets L. Goldsteins, I. Buceniaks, L. Buligins	33
D.2.3. - Analytical investigation of mhd instability in annular linear electromagnetic induction pump L. Goldsteins, A. Gailitis, L. Buligins, Y. Fautrelle, C. Biscarrat	38
D.2.4. - The ASTRID project and related R&D on NA technology C. Latge, P. Le Coz, O. Gastaldi, F. Gauche, N. Devictor.	43
D.2.5. - Acoustic MHD generator C. Gailitis	52
D.2.6. - Design of annular linear induction pump for high temperature liquid lead transportation Jae Sik Kwak, Hee Reyoung Kim	57

D.2.7. - Numerical model of induction pumps on rotating permanent magnets E.Yu. Koroteeva, M. Scepanskis, I. Buceniaks	62
D.2.8. - The viscous effects on a small MHD pump Hee Reyoung Kim	67
D.2.9. - Self-calibrating phase-shift flowmeter for liquid metals R Looney, J. Priede	71

D.3. Measuring techniques for liquid metal coolants

D.3.1. - MHD PbLi loop at IPUL S. Ivanov, A. Shishko, A. Flerov, E. Platacis, A. Romanchuks, A. Zik	76
D.3.2. - Novel induction coil sensor system for contactless inductive flow tomography M. Ratajczak, T. Wondrak, K. Timmel, F. Stefani, S. Eckert	81

D.5. Liquid metal mixing

D.5.1. - Liquid metal stirring by rotating localized magnetic field in a cylindrical container M. Rivero, S. Cuevas, E. Ramos	86
--	----

E. APPLIED MHD FOR MATERIAL APPLICATION

E.1. Metallurgical applications

E.1.1. - Application of magnetically driven tornado-like vortex for stirring floating particles into liquid metal I. Grants, D. Raebiger, T. Vogt, S. Eckert, G. Gerbeth	91
E.1.2. - Some methods for electrovortex flows control in DC arc furnaces with bottom electrode O. Kazak	96
E.1.3. - Application of MHD technology in non-ferrous metallurgy in Siberia V. Timofeev, M. Khatsayuk, G. Lybzikov, A. Avdulov	101
E.1.4. - Free surface deformation and formation of electrical discharges under current carrying fluids in magnetic fields I.B. Klementyeva, M.E. Pinchuk, I.O. Teplyakov, Abdellah Kharicha	106
E.1.5. - Influence of mhd-processes in working area of magnetodynamic installations for aluminium alloys on their operating characteristics V.I. Dubodelov, M.A. Slazhniev, Yu.V. Moyshev, K.S. Bogdan, A.D. Podoltsev, M.S. Goryuk	111
E.1.6. - The influence of processing parameters on fluid flow in continuous casting of mould with vertical electromagnetic brake Wang Engang, Li Fei	116
E.1.7. - Thermo-electric magnetic effect during solidification: in situ observation and theoretical interpretation Y. Fautrelle, G. Reinhart, O. Budenkova, H. Nguyen Thi, J. Wang	117

E.1.8. - Applications of Lorentz force techniques for flow rate control in liquid metals N. Dubovikova, C. Karcher, Y. Kolesnikov	118
E.1.9. - Influence of MHD plasma actions in casting magnetodynamic installation on homogeneity of liquid aluminium alloys and their properties in solid state S. Dubodelov, V. Sidorov, J. Skorobogatko, M. Goryuk, V. Fikssen, P. Popel, A. Narivsky	123
E.1.10. - Lorentz force sismometry: a novel technique for measuring thermo-physical properties of molten metals S. Alkhalil, A. Thess, T. Frohlich, Yu. Kolesnikov	124
E.1.11. - Effect of a superimposed DC magnetic field on an AC induction semi-levitated molten copper droplet A. Bojarevičs, T. Beinerts, I. Grants, I. Kaldre, A. Švārs, G. Gerbeth, G. Gelfgats	125
E.1.12. - Solidification process in a benchmark experiment K. Zaidat, Y. Fautrelle, L. Hachani	130
E.1.13. - Segregation control during directional solidification using magnetic field and electric current I. Kaldre, Y. Fautrelle, J. Etay, A. Bojarevics, L. Buligins	131
E.1.14. - Study of turbulence the in presence of strong electromagnetic noise in the MHD stirrer with travelling and rotating magnetic field A. Pavlinov, I. Kolesnichenko, P. Frick, E. Golbraich	136
E.1.15. - Travelling magnetic field mixing for particle dispersion in liquid metal V. Bojarevics, K. Pericleous, M. Garrido, Y. Fautrelle, L. Davoust.	140

E.2. Magneto-electrolysis

E.2.1. - Magnetic field effect on properties of galvanostatically deposited Co-Pd alloys P. Žabiński, A. Sokół, K. Mech, T. Tokarski, R. Kowalik	145
E.2.2. - Chiral catalytic activities in magnetochemical etching R. Aogaki, R. Morimoto, M. Asanuma, I. Mogi, A. Sugiyama, M. Miura, Y. Oshikiri, Y. Yamauchi	149
E.2.3. - Chiral surface formation by magnetochemical etching I..Mogi, R. Aogaki, K. Watanabe	154
E.2.4. - Demixing of an initially homogeneous solution of paramagnetic ions in inhomogeneous magnetic fields X. Yang, K. Tschulik, M. Uhlemann, S. Odenbach, K. Eckert	159
E.2.5. - How to improve the uniformity of metal deposition at vertical electrodes by electromagnetic forces G. Mutschke, S. Mühlhoff, R. Selent, X. Yang, M. Uhlemann, J. Fröhlich, S. Odenbach, K. Eckert	164
E.2.6. - Numerical simulation of the mass transfer of magnetic species at electrodes exposed to small-scale gradients of the magnetic field G. Mutschke, K. Tschulik, M. Uhlemann, J. Fröhlich	169

E.2.7. - Oxide synthesis by magneto-electrodeposition A.-L. Daltin, M. Benaissa, J.-P. Chopart	172
E.2.8. - Magneto-induced effect during Mn-doped Cu ₂ O electrocrystallization M. Benaissa, A.-L. Daltin, J.-P. Chopart	177
E.2.9. - Morphology and microstructure evolution of cobalt ferrite thin films prepared by one-step magneto-electrodeposition D. Li, A.-L. Daltin, Q. Wang, J.-P. Chopart, J. He	179

E.3. MHD in crystal growth

E.3.1. - Applied travelling magnetic field during silicon solidification in a bridgman configuration M. Cablea, A. Gagnoud, A. Nouri, Y. Delannoy, K. Zaidat	184
E.3.2. - The effects of a DC field on the orientation of Ni-based single crystal growth Y. Yang, T. Luo, Y. Li, X. Feng	185
E.3.3. - Modelling of the influence of electromagnetic force on melt convection and dopant distribution during floating zone growth of silicon A. Sabanskis, K. Surovovs, A. Krauze, M. Plate, J. Virbulis	186
E.3.4. - 3D modeling of the influence of the inductor on the phase boundaries in FZ crystal growth M. Plate, A. Krauze, J. Virbulis	191
E.3.5. - Electromagnetic flow control in the ribbon growth on substrate (RGS) process P. Beckstein, V. Galindo, G. Gerbeth	196
E.3.6. - Thermoelectrically driven MHD flow field in undercooled crystal growth A. Kao, K. Pericleous	202
E.3.7. - Control of convective flows in a rectangular crucible by a special type of electromagnetic stirring R.A. Negri, A. Popescu, M. Paulescu, D. Vizman	204
E.3.8. - Modelling of pattern formation during the melting of silicon by HF EM field K. Bergfelds, J. Virbulis, A. Krauze	209
E.3.9. - Anisotropy of flow and transition between mixing regimes in stratified EM force generated flow V. Geza, E. Baake, B. Nacke, A. Jakovics	214
E.3.10. - Modeling of melting and solidification processes of photovoltaic silicon in a traveling magnetic field K. Dadzis, G. Lukin, W. Fütterer, P. Bönisch, L. Sylla, O. Pätzold	215

E.4. Electromagnetic processing of material

E.4.1. - On the flow patterns driven by a helical permanent magnetic stirrer X. Wang, X. Na	221
--	-----

E.4.2. - MHD flow under an impact of permanent magnets driving system O. Ben-David, A. Levy, B. Mikhailovich	222
E.4.3. - Influence of MHD stirring on solidification of aluminum alloy in a cylindrical crucible S.A. Denisov, V.M. Dolgikh, S.Yu. Khripchnko, I.V. Kolesnichenko, L.V. Nikulin	227
E.4.4. - Numerical simulation of low-frequency pulsed electromagnetic force influence on the melt flow in induction crucible furnace D. Musaeva, V. Ilin, E. Baake, V. Geza	232
E.4.5. - Experimental and MHD simulation for grain refinement of alloys under low-voltage pulsed magnetic field Y. Yang, X. Feng, Y. Li, T. Luo	237
E.4.6. - Effects of pulsed magnetic field on microsegregation of solute elements in K4169 Ni-based superalloy Y. Yang, X. Feng, T. Luo, Y. Li, Y. Teng	238
E.4.7. - On the influence of MHD flow parameters on the ingots structure A. Kapusta, B. Mikhailovich, S. Khripchenko, L. Nikulin	239
E.4.8. - Investigation of hydrodynamics of alumina oxide melt in a cold crucible at continuous melting and discharging V. Kichigin, V. Geza, B. Nacke, I. Pozniak	242
E.4.9. - Local Lorentz force velocity using small-size permanent magnet systems D. Hernández, C. Karcher, A. Thess	247

E.5. Electromagnetic levitation

E.5.1. - Model experiment validating the feasibility of a permanent magnet stirrer for large-scale metal melting furnaces A. Bojarevičs, T. Beinerts, M. Sarma, Yu. Gelfgat	251
E.5.2. - Numerical simulation of electromagnetic levitation in a cold crucible furnace S. Spitans, E. Baake, A. Jakovics, H. Franz	256
E.5.3. - 3D LES two-phase flow simulation of conventional electro-magnetic levitation melting experiment S. Spitans, E. Baake, B. Nacke, A. Jakovics	261

E.6. Magneto static

E.6.1. - Numerical modeling of gas bubble dynamics in liquid metal in applied DC magnetic field A. Tucs, S. Spitans, A. Jakovics, E. Baake	266
---	-----

F. FERRO FLUID
F.1. Magnetic liquids

F.1.1. - Pore scale simulation of magnetosolutal microconvection in ferrofluid saturated porous structures D. Zablotsky, D. Blums	271
F.1.2. - Surface shape of a magnetic fluid bridge between plates in the field of an electromagnetic coil T. Volkova, V. Naletova, V. Turkov	276
F.1.3. - Magnetite/oleic acid nanoparticles possessing immobilized antitumour tetrahydroisoquinoline derivatives I. Segal, A. Zablotskaya, M. Maiorov, D. Zablotsky, E. Blums, E. Abele, I. Shestakova	278
F.1.4. - Segregation in the dipolar hard sphere system: numerical simulation A.A. Kuznetsov, A.F. Pshenichnikov	283
F.1.5. - Preparation and properties of platinum coated magnetite nanoparticles G. Kronkalns, M. Maiorov, V. Serga, A. Cvetkovs, A. Krumina, D. Karashanova	288
F.1.6. - Magnetic fluid nanoparticle fractionation: experiments and sample analysis M. Maiorov, A. Mezulis	293
F.1.7. - Ferrofluid bridge between two cones and a cylinder in the magnetic field of a line conductor A.S. Vinogradova, V.A. Naletova	297
F.1.8. - The experimental study of the motion of elongated bodies with magnetizable material in rotating magnetic field D.A. Pelevina, V.A. Turkov, M.V. Lukashevich, S.A. Kalmykov, V.A. Naletova	302
F.1.9. - Experimental investigation of magnetic nanoparticle transfer within a porous medium and under influence of a magnetic field V. Sints, E. Blums, M. Maiorov, G. Kronkalns, O. Petricenko	306
F.1.10. - 100 μm thick ferrofluid layer as a resettable memory cell I. Pukina, A. Mezulis, D. Zablotsky	311
F.1.11. - Experimental study of initiation of convection in a spherical cavity filled with nanofluid A.A. Bozhko, M.T. Krauzina, G.F. Putin, S.A. Suslov	316
F.1.12. - Diffusion coefficient of a ferrofluid-water system in a Hele-Shaw cell G. Kitenbergs, R. Perzynski, A. Čēbers, K. Ērglis	321
F.1.13. - Deformation of a body with a magnetizable polymer in a uniform magnetic field V.A. Naletova, D.I. Merkulov, I. Zeidis, K. Zimmermann	322
F.1.14. - Waves in ferrofluid convection induced by inclined magnetic field A. Sidorov, S. Suslov, H. Rahman, G. Putin, A. Bozhko	326

F.1.15. - Dynamical properties of transformer oil based magnetic fluids M. Rajnak, J. Tothova, J. Kovac, J. Kurimsky, B. Dolnik, P. Kopčanský, M. Molcan, F. Royer, M. Timko	327
F.1.16. - Experimental testing of the mass exchange on the ferrofluid surface A. Lickrastina, M. Maiorov, E. Blums	332
F.1.17. - Increase of the sensitivity of liquid crystals to magnetic field due to doping with magnetic nanoparticles P. Kopčanský, N. Tomašovičová, M. Timko, V. Gdovinová, T. Tóthkatona, N. Éber, C.-K. Hu, S. Hayryan, X. Chaud	337
F.1.18. - Numerical study of magnetic field driven micro-convection in the Hele-Shaw cell A. Tatulcenkovs, G. Kitenbergs, K. Ērglis, A. Cēbers	342
F.1.19. - Experimental study on forced convective heat transfer and flow resistance of magnetic fluid flow under non-uniform magnetic field M. Motozawa, S. Tatsuno, T. Sawada, Y. Kawaguchi, M. Fukuta	346
F.1.20. - Stability analysis of a particle with a finite energy of magnetic anisotropy in a rotating and precessing magnetic field J. Čimurs, A. Cēbers	351

F.2. Electrohydrodynamics

F.2.1. - Deformation of a double-layer drop in an alternating electric field D.I. Kvasov, V.A. Nalotova	356
--	-----

F.3. Magnetorheological suspensions

F.3.1. - Diffusion of magnetotactic bacteria in rotating magnetic field R. Taukulis, A. Cēbers	361
---	-----

INCREASE OF THE SENSITIVITY OF LIQUID CRYSTALS TO MAGNETIC FIELD DUE TO DOPING WITH MAGNETIC NANOPARTICLES

KOPČANSKÝ¹ P., TOMAŠOVIČOVÁ¹ N., TIMKO¹ M., GDOVINOVÁ¹ V., TÓTH-KATONA² T., ÉBER² N., HU³ C.-K., HAYRYAN³ S., CHAUD⁴ X.

¹Institute of Experimental Physics, Slovak Academy of Sciences, Watsonova 47, 040 01 Kosice, Slovakia, kopcan@saske.sk

²Research Institute for Solid State Physics and Optics, Wigner Research Centre for Physics Hungarian Academy of Sciences, H-1525 Budapest, P.O.Box 49, Hungary

³Institute of Physics, Academia Sinica, 128 Sec.2, Academia Rd., Nankang, Taipei 11529, Taiwan

⁴High Magnetic Field Laboratory, CNRS, 25 Avenue des Martyrs, Grenoble, France

Abstract: The contribution is an overview of the observations regarding the structural transitions in ferronematics based on thermotropic nematics doped with magnetic nanoparticles of different shape, and the magnetic field induced shift of the isotropic to nematic phase transition temperature. Due to presence of magnetic particles an increase of the isotropic-nematic phase transition temperature was observed as a function of applied magnetic field. The response of ferronematics to very low magnetic fields is also presented which is important for the construction of various magneto-optical devices.

1. Introduction

Liquid crystals can be oriented by electric or magnetic fields due to the anisotropy of the dielectric permittivity or the diamagnetic susceptibility [1]. As the former is in the order of unity, in conventional devices the driving voltages are in the order of a few volts. However, because of the small value of the anisotropy of the diamagnetic susceptibility ($\sim 10^{-7}$), the magnetic field necessary to realign liquid crystals have to reach rather large values ($B \sim 10T$ depending on the thickness of the liquid crystal layer). In an effort to enhance the magnetic susceptibility of liquid crystals, the idea of doping them with small amount of tiny magnetic particles was theoretically introduced by Brochard and de Gennes [2]. They have developed the continuum theory of magnetic suspensions in nematic liquid crystals (ferronematics). In their theoretical work rod-like magnetic particles with the length $L \gg a$ (where a is the molecular size of the nematic liquid crystal) and with a diameter of $d \sim L/10$ were considered. The volume concentration of magnetic particles was supposed to be sufficiently small ($\sim 10^{-4}$) in order to be able to ignore the inter-particle magnetic dipole-dipole interaction. They predicted that a rigid anchoring with $m \parallel n$ would result in the ferromagnetic behaviour of the mixture. Here the unit vector n (the director) describes the preferential direction of the nematic molecules and the unit vector m denotes the orientation of the magnetic moment of the magnetic particles. In the first experimental paper, Rault et al. [3] reported about the basic magnetic properties of a suspension of rod-like γ - Fe_2O_3 particles in the liquid crystal MBBA. In order to stabilize the suspension, the particles were first coated with a surfactant and then mixed with the nematic liquid crystal. The obtained results confirmed the existence of a ferromagnetic state in such suspension. Additionally they have found that the temperature of the nematic-isotropic transition decreases with increasing volume concentration of particles. Later, based on the estimations given in [2], first lyotropic [4,5] and then thermotropic [6] ferronematics have been prepared and studied. These experiments confirmed the existence of considerable orientational and concentrational effects in liquid crystals doped with magnetic particles, but raised a lot of questions as well.

One of the most important questions solved in the theory of ferronematics is the problem of the equilibrium orientation of magnetic particle, i.e. the direction of its magnetic moment m ,

in the nematic matrix. The Brochard and de Gennes theory [2] considers the rigid anchoring with m parallel with n . Based on later experiments, which excluded the co-alignment of m and n in some thermotropic ferronematics, the Burylov and Raikher's theory was constructed [7-9]. This theory considers the finite value of the surface density of the anchoring energy W at the magnetic particle - nematic boundary. The finite value of W , as well as the parameter $\omega=Wd/K \leq 1$, characterize the soft anchoring of nematic molecules on the surfaces of magnetic particles (d - typical size of magnetic particle, K - corresponding Frank orientation-elastic modulus of liquid crystal). The soft anchoring, unlike the rigid one, permits both types of boundary conditions ($m \perp n$ and $m \parallel n$), thus the Burylov and Raikher's theory could explain the experimental findings. In the frame of this theory the instabilities of the uniform texture in ferronematics exposed to external magnetic or electric field (Fréedericksz transitions) were analysed and the expressions for their critical fields in different geometries were derived.

2. Results

The studied ferronematic samples were based on the thermotropic nematic 4-(trans-4'-n-hexylcyclohexyl)-isothiocyanatobenzene (6CHBT). 6CHBT is an enantiotropic liquid crystal with high chemical stability [10]. The temperature of the nematic-to-isotropic transition (the clearing point) of the studied nematic is $T_{NI} = 42.8^\circ\text{C}$. The nematic samples were doped with different kind of magnetic particles in volume concentration of 2×10^{-4} . The synthesis of magnetic particles of various shape was described in [11]. The size of spherical particles was 11.6nm; the diameter and the length of rod-like particles were 25nm and 1200nm, respectively. The length of chain-like particles was approximately 400nm; the size of a single particle in the chain was 34nm.

The structural transitions in ferronematic samples were monitored by capacitance measurements in a capacitor made of ITO-coated glass electrodes (LINCAM Co.). The capacitor with an electrode area of approximately $1\text{cm} \times 1\text{cm}$ was connected to a regulated thermostat system; the temperature was stabilized with the accuracy of 0.05°C . The distance between the electrodes (sample thickness) was $D = 5\mu\text{m}$. The capacitance was measured at the frequency of 1kHz by a high precision capacitance bridge Andeen Hagerling. The stability of the samples in the strong magnetic fields was verified by repeating the capacitance measurements after 5 months on the same samples, with reproducible results.

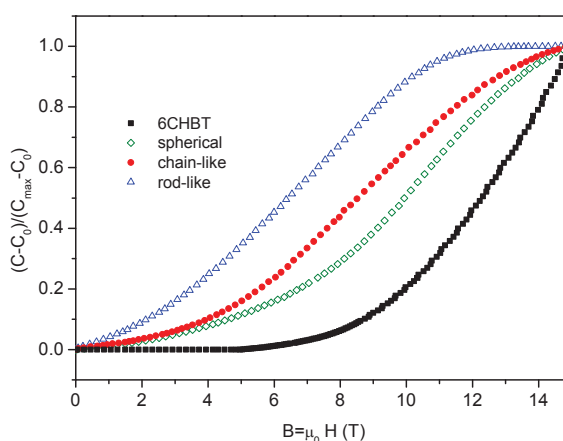


Figure 1: Reduced capacitance dependence of undoped 6CHBT and 6CHBT doped with spherical particles, chain-like particles and rod-like particles on external magnetic field measured at $U_B = 10\text{V}$ (C_0 and C_{max} are the capacitance at $B=0$ and at B which restores the planar alignment, respectively).

The ferronematics based on the magnetic particles of various shape [11] were subjected to the combined action of electric and magnetic fields at the temperature of 35 °C. The magnetic field was applied perpendicular to E. Fig. 1 exhibits the dependence of the dimensionless reduced capacitance on the magnetic field at a bias voltage of 10V for undoped 6CHBT as well as for 6CHBT doped with magnetite particles of different shape. Doping with magnetic nanoparticles evidently reduces the critical field, confirming that the coupling between the director and the magnetic moment favours $m \parallel n$. The reduction is the smallest for spherical particles and the largest for rod-like particles. It has been concluded [11] that the larger shape anisotropy of the particles changes the character of the anchoring at the liquid crystal – particle interface from soft to rigid. The presented results show that doping with magnetic particles shaped similarly to the molecules of the host liquid crystal is more effective and thus offer better perspectives for ferronematics in applications where the magnetic field is necessary to control the orientation of the liquid crystal.

Another interesting phenomenon in liquid crystals is the possibility to alter the isotropic to nematic phase transition with external field [12-14]. However, the effect could not be induced by magnetic-field [15] until recently [16]. The principal reason is that the estimated critical fields are well over 100 T for traditional liquid crystal materials [15]. The first experimental observation of the predicted magnetic-field dependence of the nematic-isotropic phase transition temperature has been recently carried out [16] on a powerful electromagnet (B up to 30T). To demonstrate the effect, besides the powerful electromagnet, the proper choice of a „non-conventional” (bent-core) nematic liquid crystal material was also necessary. The „non-conventional” nematic material chosen in Ref. [16], has considerably different physical properties compared to „conventional” calamitic nematics; the first-order character of the nematic-isotropic transition at the „clearing point” is substantially weaker than that for „conventional” nematics. These properties, combined with the high magnetic field have contributed to the observation of the phase transition temperature shift of $\sim 0.8^\circ\text{C}$ at the magnetic field of 30T.

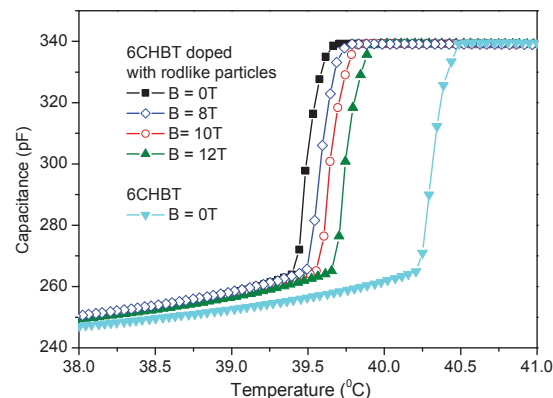


Figure 2: Capacitance vs. temperature for undoped 6CHBT and 6CHBT doped with rodlike magnetic particles measured at different magnetic fields.

The influence of the magnetic particles on the magnetic field induced isotropic-nematic phase transition was also studied in a “conventional” calamitic liquid crystal 6CHBT by capacitance measurements [17]. The used magnetic particles were either spherical or rod-like. In both cases the size of the magnetic particles was much greater than the dimensions of the liquid crystal molecules, i.e. the magnetic particles can be regarded as macroscopic objects floating in the liquid crystal. The surface of the magnetic particles is able to orient the adjacent liquid

crystal molecules. During the measurements the magnetic field was applied parallel with the capacitor electrodes.

Our results have confirmed that the shape of the magnetic particles affects the phase transition from the isotropic phase. In the pure 6CHBT as well as in 6CHBT doped with spherical magnetic particles no measurable field induced shift of the isotropic-nematic phase transition temperature was observed in magnetic fields up to 12T. On the contrary, in 6CHBT doped with rodlike magnetic particles (diameter size 10 nm, length 50 nm and volume concentration 2×10^{-4}) a shift of 0.25°C was found in the phase transition temperature at 12T (Fig. 2). Therefore, our results have proven that ferronematics composed of calamitic liquid crystals and rod-like magnetic nanoparticles can be just as effective in demonstrating the magnetic field induced isotropic-nematic phase transition as bent-core nematics [16].

In recent works by Podoliak et al. [18], and Buluy et al. [19] both experimental and theoretical investigations have been reported about the optical response of suspensions of ferromagnetic nanoparticles in nematic liquid crystals on the imposed magnetic field. The authors have measured a linear optical response in ferronematics at very low magnetic fields (far below the threshold of the Freedericksz transition). A similar effect was also observed in our dielectric measurements in samples doped with spherical [20] or rod-like [21] magnetic particles as it is demonstrated in Fig.3. The figure provides a clear evidence for a nearly linear magnetic field dependence of the capacitance in the low magnetic field region.

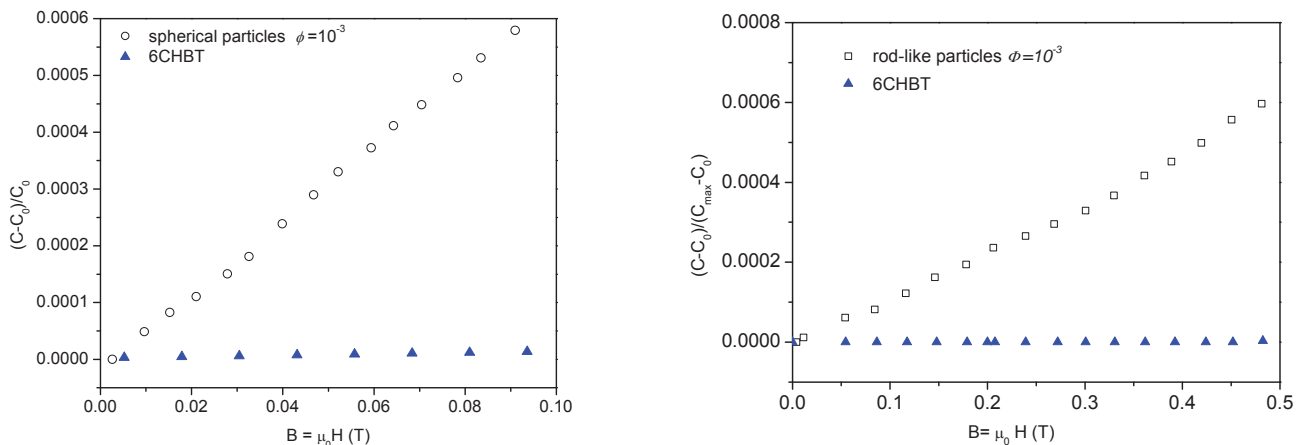


Figure 3: Reduced capacitance versus magnetic field for undoped 6CHBT and for 6CHBT doped with spherical particles and rod-like particles.

3. Conclusion

We have shown, that doping liquid crystals with magnetic nanoparticles increases the sensitivity to external magnetic field. The shape and the size of the magnetic nanoparticles play significant role in structural transitions. We have observed an increase of the isotropic-nematic phase transition temperature in ferronematics based on the calamitic liquid crystals doped with magnetic nanoparticles in magnetic field of $\sim 10\text{T}$. Moreover, the magnetic particles can influence the response of liquid crystals also in the low magnetic field region, far below Fréedericksz transition.

Acknowledgements.

This work was supported by the project VEGA 0045, the Slovak Research and Development Agency under the contract No. APVV-0171-10, Ministry of Education Agency for Structural Funds of EU in frame of projects 26220120021, 26220120033 and 26110230097, the GHMFL (CRETA), the Hungarian Research Fund OTKA K81250, and M-era.Net – MACOSYS (OTKA NN110672).

4. References

- [1] de Gennes, P.G.; *The Physics of Liquid Crystals*, (Clarendon Press, Oxford 1974)
- [2] Brochard, F.; de Gennes, P.G.; (1970) Theory of magnetic suspensions in liquid crystals, *J.Phys. (Paris)* 31, 691
- [3] Rault, J.; Cladis, P.E.; Burger, J.P.; (1970) *Ferronematics*, *Phys.Lett. A* 32, 199
- [4] J. Liebert, A. Martinet, (1979) Coupling between nematic lyomesophases and ferrofluids, *J.Phys.Lett.* 40, 363
- [5] A.M. Figueiredo Neto, L. Liebert, A.M. Levelut, (1984) Study of ferrocholesteric discotic and calamitic lyotropics by optical microscopy and X-ray diffraction, *J.Phys. (Paris)* 45, 1505
- [6] S.H. Chen, N.M. Amer, (1983) Observation of macroscopic collective behaviour and new texture in magnetically doped liquid crystals, *Phys.Rev.Lett.* 51, 2298
- [7] S.V.Burylov, Y.L.Raikher, (1990) On the orientation of an anisometric particle suspended in a bulk uniform nematic, *J.Phys.Lett. A* 149, 279
- [8] S.V.Burylov, Y.L.Raikher, (1993) Magnetic Fredericksz transition in a ferronematic, *J.Magn.Magn.Mater.* 122, 62
- [9] S.V.Burylov, Y.L.Raikher, (1995) Macroscopic properties of ferronematics caused by orientational interactions on the particle surfaces. 1.Extended continuum model, *Mol.Cryst.Liq.Cryst.* 258, 107
- [10] Dabrowski, R.; Dziaduszek, J.; Szczucinski, T.; (1984) 4-(Trans-4-n-Alkylcyclohexyl)isothiocyanatobenzenes a new class of low-melting stable nematics, *Mol.Cryst.Liq.Cryst.Lett.* 102, 155
- [11] Kopčanský, P.; Tomašovičová, N.; Koneracká, M.; Závaišová, V.; Timko, M.; Džarová, A.; Šprincová, A.; Éber, N.; Fodor-Csorba, K.; Tóth-Katona, T.; Vajda, A.; Jadzyn, J.; (2008) Structural changes in the 6CHBT liquid crystal doped with spherical, rodlike, and chainlike magnetic particles, *Phys Rev E* 78, 011702
- [12] Helfrich, W.; (1970) Effect of electric fields on the temperature of phase transition of liquid crystals, *Phys. Rev. Lett.* 24, 201
- [13] Lelidis, I.; Durand, G.; (1993) Electric-field-induced isotropic-nematic phase transition, *Phys. Rev. E* 48, 3822
- [14] Stanley, H.; *Introduction to Phase Transitions and Critical Phenomena*, Oxford Science, New York, 1971
- [15] Rosenblatt, C.; (1981) Magnetic field dependence of nematic-isotropic transition temperature, *Phys. Rev. A*.24, 2236
- [16] Ostapenko, T.; Wiant, D.B.; Sprunt, S.N.; Jáklí, A.; Gleeson, J.T.; (2008) Magnetic- field induced isotropic to nematic liquid crystal phase transition, *Phys. Rev. Lett.* 101, 247801/1-4
- [17] Kopčanský, P.; Tomašovičová, N.; Koneracká, M.; Závaišová, V.; Timko, M.; Hnatič, M.; Éber, N.; Tóth-Katona, T.; Jadzyn, J.; Honkonen, J.; Beaugnon, E.; Chaud, X.; (2011) Magnetic-field induced isotropic to nematic phase transition in ferronematics, *IEEE Transactions on Magnetics* 47, 4409.
- [18] Podoliak, N.; Buchnev, O.; Buluy, O.; D'Alessandro, G.; Kaczmarek, M.; Reznikov, Y.; Sluckin, T.J.; (2011) Macroscopic optical effect in low concentration ferronematics, *Soft Matter* 7, 4742-4749.
- [19] Buluy, O.; Nepijko, S.; Reshetnyak, V.; Ouskova, E.; Zadorozhnii, V.; Leonhardt, A.; Ritschel, M.; Schonhense, G.; Reznikov, Y.; (2011) Magnetic sensitivity of a dispersion of aggregated ferromagnetic carbon nanotubes in liquid crystals, *Soft Matter* 7, 644-649.
- [20] Tomašovičová, N.; Timko, M.; Mitróová, Z.; Koneracká, M.; Rajňak, M.; Éber, N.; Tóth-Katona, T.; Cahud, X.; Jadzyn, J.; Kopčanský, P.; (2013) Capacitance changes in ferronematic liquid crystals induced by low magnetic fields, *Phys. Rev E* 87, 014501
- [21] Kopčanský, P.; Tomašovičová, N.; Tóth-Katona, T.; Éber, N.; Timko, M.; Závaišová, V.; Majorošová, J.; Rajňak, M.; Jadzyn, J.; Chaud, X.; (2013) Increasing the magnetic sensitivity of liquid crystals by rod-like magnetic nanoparticles, *Magnetohydrodynamics* 48, 407-413